Analysis of the maximum friction condition for green body forming in an ANSYS environment

Facchinetti, Maurizio; Miszuris, Wiktoria

Published in:
Journal of the European Ceramic Society

DOI:
10.1016/j.jeurceramsoc.2016.01.040

Publication date:
2016

Citation for published version (APA):
Facchinetti, M., & Miszuris, W. (2016). Analysis of the maximum friction condition for green body forming in an ANSYS environment. *Journal of the European Ceramic Society*, *36*(9), 2295-2302. https://doi.org/10.1016/j.jeurceramsoc.2016.01.040

Analysis of the maximum friction law for green body forming in ANSYS environment.

Maurizio Facchinetti[1], Wiktoria Miszuris[2]

[1] EnginSoft Bergamo (Italy), Via Stezzano, 24126 Bergamo BG, Italy

[2] Department of Mathematics, Aberystwyth University, SY23 3BZ, Wales, UK

Abstract

Axisymmetric extrusion of elasto-plastic material with the maximal shear stress condition between the material and the forming tool is considered. Elastic component of the deformation is assumed negligible smaller in comparison with its plastic part. Challenges related to numerical modeling of such problem with the commercial software ANSYS are identified. Recommendations to treat the problem have been drawn.

Keywords: green body, forming process, maximal friction law, singular strain, ANSYS

1. Introduction

Cold powder compaction leading to a mechanical densification of the granular material with its subsequent sintering completes the treatment and yields the desired shape of the ceramics possessing required mechanical properties [1-3]. A critical issue to eliminate waste in the ceramic production is to be able to properly model the entire production process. On the stage of the material compactness, the constitutive elasto-plastic models are required for modelling of the process [4-13]. Various phenomenological models have been proposed there so far. Some of them incorporate also friction phenomenon and lead to the singular yield surfaces that required a special cure for the applied numerical procedure [14.15].

Friction is the other of the crucial phenomena in the forming processes of different materials and requires proper description within the computational modeling [16]. Such processes, in turn, constitute one of the main technological processes in production of ceramics. Moreover, any micro-defect appearing on the stage of the green body forming may lead to unrecovered waste in the further production process.

In the case of the maximum friction law, the friction surface can be a source of singular behavior of rigid plastic solutions [17-19] and thus may be a source of further fracturing due to the microstructure inhomogeneity. This singular behaviour is demonstrated by the normal component of the strain rate tensor near the maximum friction surface (maximum in the sense - maximum possible within the plastic flow rule).

The maximum friction surface is a source of singular solution behaviour for several rate-independent plasticity models. In case of the conventional viscoplastic law, the singularity does not appear while the sliding condition is no longer valid and sticking occurs [20]. However, it has been recently revealed that viscoplastic law with saturation together with the maximum friction law on the boundary may lead to the same overall results (sliding condition with the pronounced strain singularity) as for the case of classic plastic material with constant yield stress [21-22].

Even though such singular behavior can be directly implemented into the numerical scheme for some simple geometry [23, 24] that allowed to analyse some specific features of the process,

Finite Element method becomes now the most efficient tool for modeling various technological processes including ceramic production [25-31]. However, if one need to incorporate the maximum friction law in the compactness process, aforementioned singular strain behavior causes essential difficulties. Therefore, it is of fundamental importance to incorporate the fundamental properties of the solutions obtained for boundary value problems involving the maximum friction law into the FEM software or, at least, to estimate how available existing options allow one to obtain meaningful computational results. This work is concentrating on performace of the popular FEM commercial code ANSYS [32] to tackle the problems of that class.

2. Most Common Friction Laws

Various different friction laws are commonly used in commercial FEM codes to define for the boundary conditions. The most common are listed in the following:

a) Stick condition (tangent velocity is equal to zero at the boundary). This is one of the simplest laws. It used frequently in polymer forming processes [32].
b) Slip with shear force depending on shear velocity at the wall (with function given by user). These are normally empirical laws mainly based on experimental data valid for single materials undergoing large plastic deformation with an extremely law yield stress.
c) Coulomb law is probably the most popular in contact problems with friction [16]. This is a law of the form:

$$\tau = \mu\sigma_n \,, \tag{1}$$

where τ is the friction stress, μ is the friction coefficient and σ_n is the normal stress measured at the boundary. This is a law commonly used in commercial software like ANSYS and others. Solutions as Coulomb law can sometimes give unrealistically high friction stresses and/or be incompatible with the yield functions.
d) For this reasons, the Tresca law was introduced (originally by researchers dealing with metal forming) and is now the most popular law in modeling of various forming problems. The Tresca law can be written in the form:

$$\tau = m\tau_{max} \,, \tag{2}$$

Here again, τ is the friction stress, while $0 \leq m \leq 1$ is the Tresca coefficient and τ_{max} is the maximum shear stress measured at the boundary which is allowed by the plastic yield condition (also called yield shear stress). In case of $m = 0$ one deals with the frictionless contact, while in case $m = 1$, equation (2) determines the maximum shear stress according to the used yield condition which is prescribed along the boundary.

When $m = 1$, the respective solution can exhibit a singular behavior near the surface (according to the theory [17] one can expect infinite strain rate at the boundary at least for the rigid plastic materials). Moreover, it is difficult to predict what type on the deformation conditions are

compatible with the process in each point of the interface (both sticking and sliding conditions are possible depending on what the yield condition). Moreover, in case of sticking the strain rate is no longer singular along the boundary but may demonstrate a very high concentration. We try to understand how commercial FEM software like ANSYS behaves in such cases.

3. FEM model for forming simulations

Different geometries and settings were tried during the implementation of the model. Only the final ones are presented here, although some results on preliminary models will also be shown for explanation purposes.

3.1 Geometry, materials, program settings

The forming simulations were performed on the simple axisymmetric geometry shown in Figure 1, which includes the part that has to be formed and a rigid mold. For the part to be molded, different material properties were implemented: practically rigid - perfectly plastic material (to be more accurate it was a material with an extremely very high Young modulus) and elasto plastic material with von Mises yield criterium and different tangent modulus after yielding (bilinear kinematic hardening).

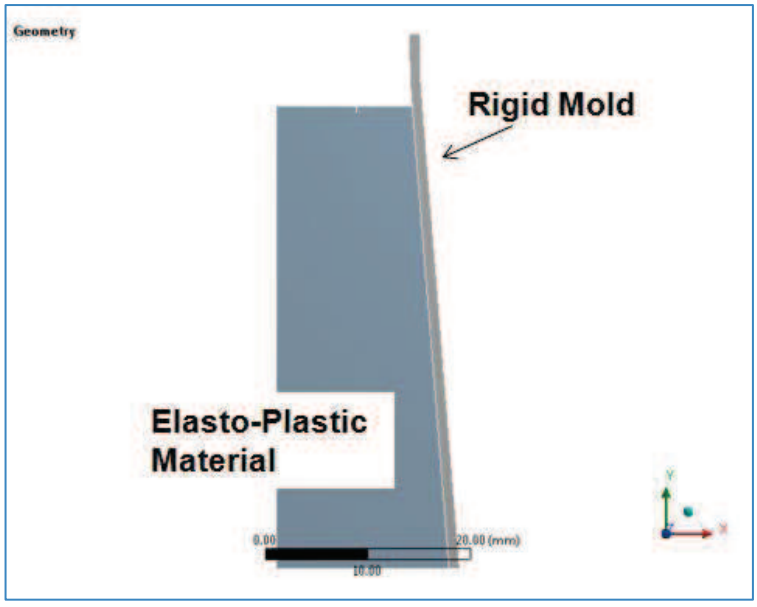

Figure 1: Axisymmetric extrusin of the elastoplastic material. Geometry of the model.

Transient structural analyses were performed with "large strain" option activated, since the material undergoes large deformations during forming and we have to take into account stiffness changes that result from changes in an element's shape and orientation. To obtain convergence, smaller time steps were set at the starting part of simulations.

3.2 Boundary conditions, contact settings

Boundary conditions applied are shown in Figure 2. First kinematic boundary condition was applied at lower boundary of the deformable body (more accurately it was 5 mm displacement in 1 s).

The symmetry condition was prescribed on the axis of symmetry. Frictional contact was imposed between the deformable body and the rigid mold, except at the upper part of the mold where

frictionless contact was imposed, to facilitate convergence. A pure-penalty method for the contact detection was used in ANSYS environment.

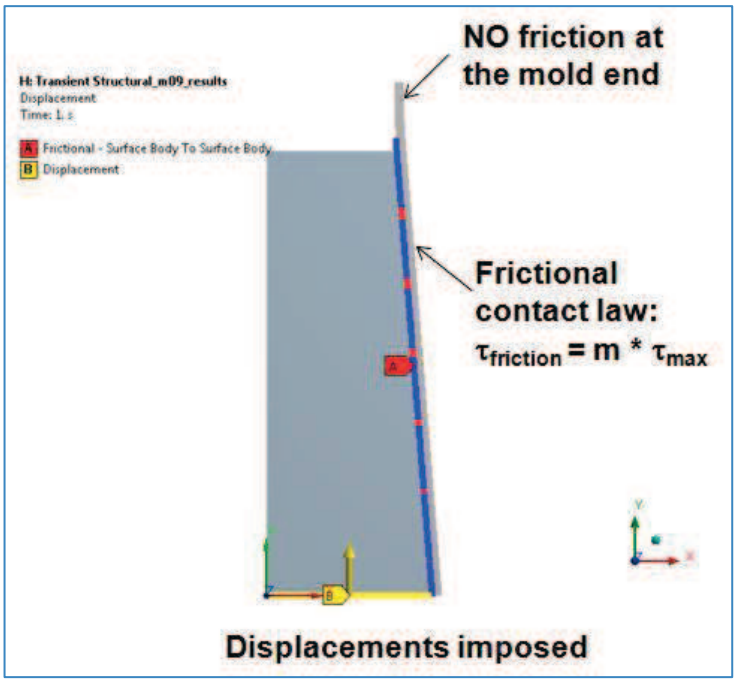

Figure 2: Boundary conditions emposed on different sides of the domain.

The friction along the contact was prescribed by the Tresca law with different values of the coefficient *m*. Note that imposing such a friction law in ANSYS environment is not trivial task. Normally Coulomb law is used by the program, as shown in Figure 3 where it is possible to fix a limit value of friction stress through a proper choice of a parameter called TAUMAX. Using this parameter and parameter COHE large anough to garantee that the only TAUMAX regime is practically considered it is possible to make friction stress *independent from the applied contact pressure p.*

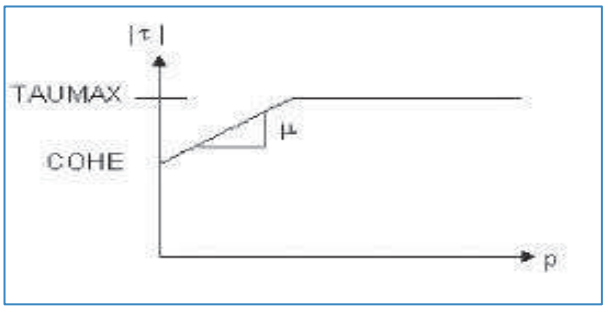

Figure 3; Relashonship between friction stress at the boundary and pressure applied during slipping in ANSYS environment

In ANSYS, or more accurately in its standard use, the TAUMAX parameter is considered as a given costant, while in the Tresca law the friction stress normally is not a constant but depends on the max shear stress calculated at different positions on the boundary.

In present simulations TAUMAX is written in table format as a function of coordinates. For each mesh node on the boundary the coordinates are extracted and so the maximum shear stress. As a result, the friction stress is calculated through the formula (2) and those values were assigned on the

boundary contact elements (different values at different positions). This operation is performed for each substep of the calculations. Since getting max shear stress is a post-processing operation performed at the end of substep, while assigning friction stress on contact is a pre-processing operation, this requires a RESTART at each substep (through RESCONTROL command) in ANSYS environment. All these operations are performed through an APDL (ANSYS parametric design language) macro suitably built.

3.3 Mesh Settings

As regards to the mesh settings, different element types were analyzed during model development. Quadratic axisymmetric elements PLANE 183 (default for ANSYS) gave better convergence for high values of Tresca coefficient *m*, considering approximately the same number of degree of freedom. More elements were placed near the mold wall where higher velocity gradients are expected, (see Figure .

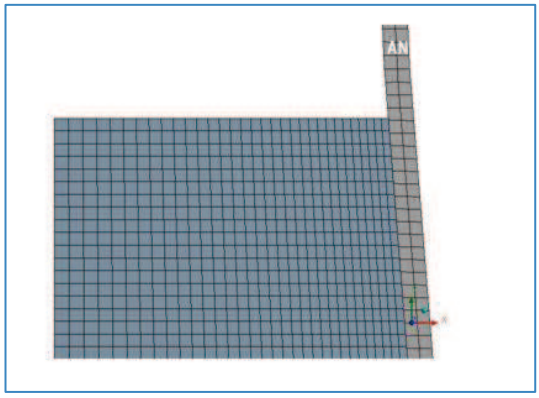

Figure 4: Mesh used in computations. Size of the elements was adjusted for different values of the Tresca parameter *m* to garantee convergence.

The size of the elements in the mesh was chosen to guarantee the convergence of results, in other words, we checked that the difference in results obtained between two different meshes become negligible.

Actually, for low values of the Tresca parameter *m* (for example m = 0.5) there were no real differences in results obtained using a coarse or a fine meshes. However, with high values of *m* (0.9 or larger) there were essential differences in the velocities and the strain rates near the mold wall for different meshes. Moreover, as one could expect from the near singular behavior near the boundary, it was extremely difficult to trace the strain rate values near the mold wall with a coarse mesh (see Figure) where the mesh had to reassign to be fine enough to follow the values of the strain rate near the mold wall with $m > 0.9$.

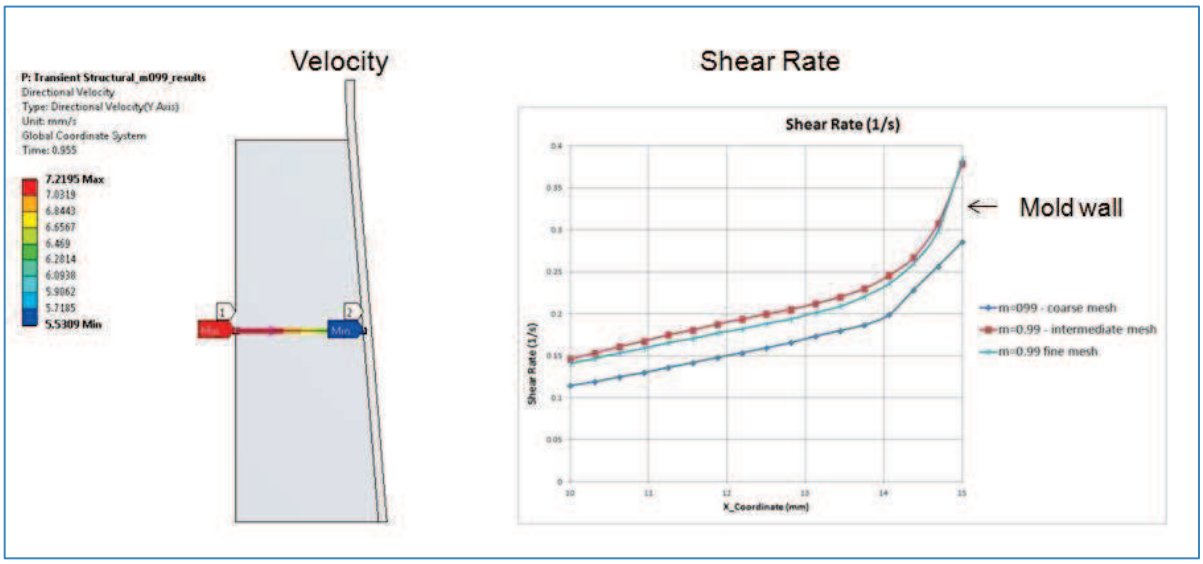

Figure 5: Shear rate trend along the indicated path (from the point lying at the axis of symmetry to the external boundary) for three different meshes.

4. Numerical results

For the final model, three different materials were used.

4.1. Rigid- perfectly plastic model.

The first material was will refer as the rigid-perfectly plastic one. It was implemented by choosing the standard bilinear elasto-plastic model with a very high value of the Young modulus (more than $2 \cdot 10^5$ MPa) while the value of the constant kinematic hardening was only 50 MPa.

Figure shown both, the initial and the final, positions of the deformed material, while Figure demonstrates the plastic strain for the same model. The level of elastic strain was negligible in comparison with the plastic one and thus not presented.

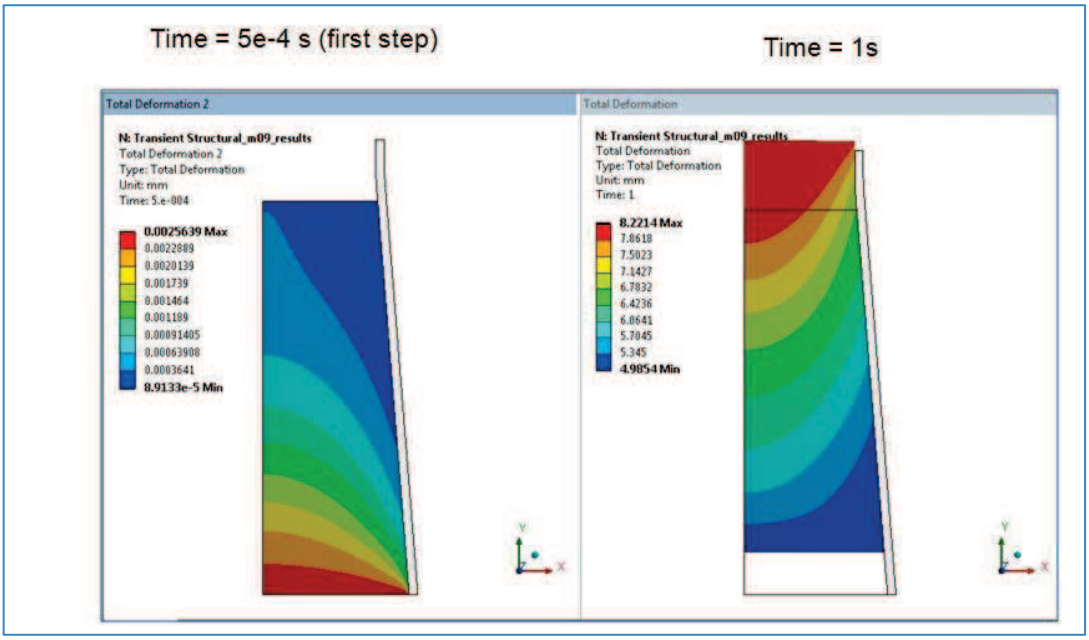

Figure 6: Displacement distrubution at initial and final stage of the process for the rigid-perfectly plastic material.

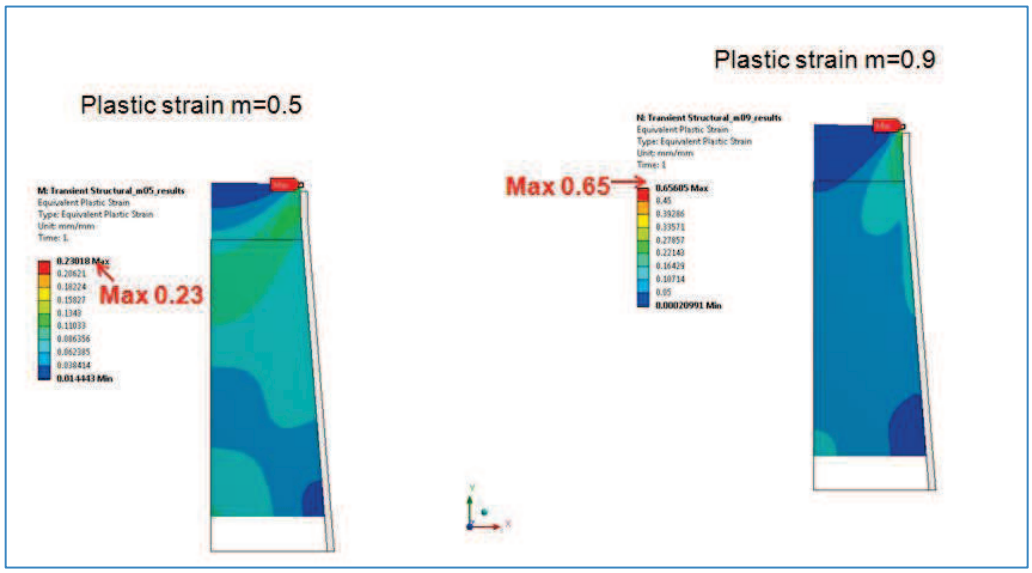

Figure 7: Plastic strain with $m = 0.5$ and $m = 0.9$ for the rigid-perfectly plastic material.

Figure displays the vertical (y-direction) velocities computed for two different values of the Tresca parameter $m = 0.5$ and $m = 0.9$ at the final stage of the deformation process. Note the difference in velocity isolines for $m = 0.5$ and $m = 0.9$. It is clearly seen that the variation of vertical velocity near the mold is much higher for the case $m = 0.9$.

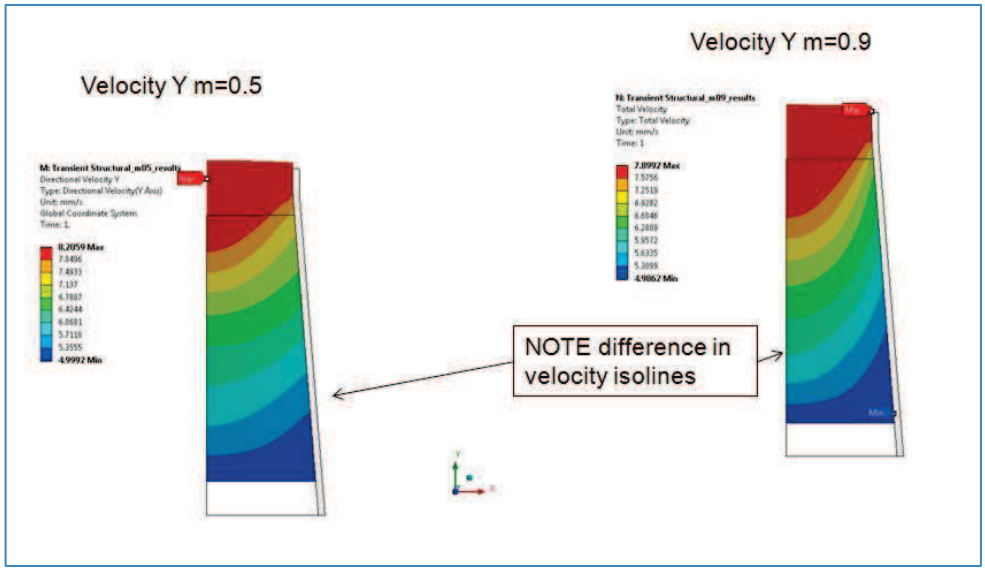

Figure 8: Vertical velocities at the final stage of the plastic deformation for two different values of the Tresca parameter $m = 0.5$ and $m = 0.9$ for the rigid-perfectly plastic material.

In Figure 9 we present the profiles of the vertical velocities alongh the defined path in the middle part of the domain for different Tresca parameter values: $m = 0.5; 0.9; 0.95; 0.98; 0.99; 0.995$).

Figure 4 shows the distrubution of the shear component of the strain rate along the same path for different values of Tresca parameter m. As m approaches it maximum ($m = 1$), the component of the strain rate increases near the mold wall while the convergence of the computations becomes difficult to preserve and the program finally crashes when the programe can no longer preserve the imposed boundary condition (and the sliding regime along a small part of the external boundary changes to the sticking one).

However, for the value close enough to the maximun (m = 0.995), ANSYS provides reasonable results. Moreover, one can observe that the shear component of the strain rate tenson demonstrates behaviour close to $1/\sqrt{s}$ where s is the distance to the mold wall. This fact fully coinsides with the theoretical predisction [17-19] for such material.

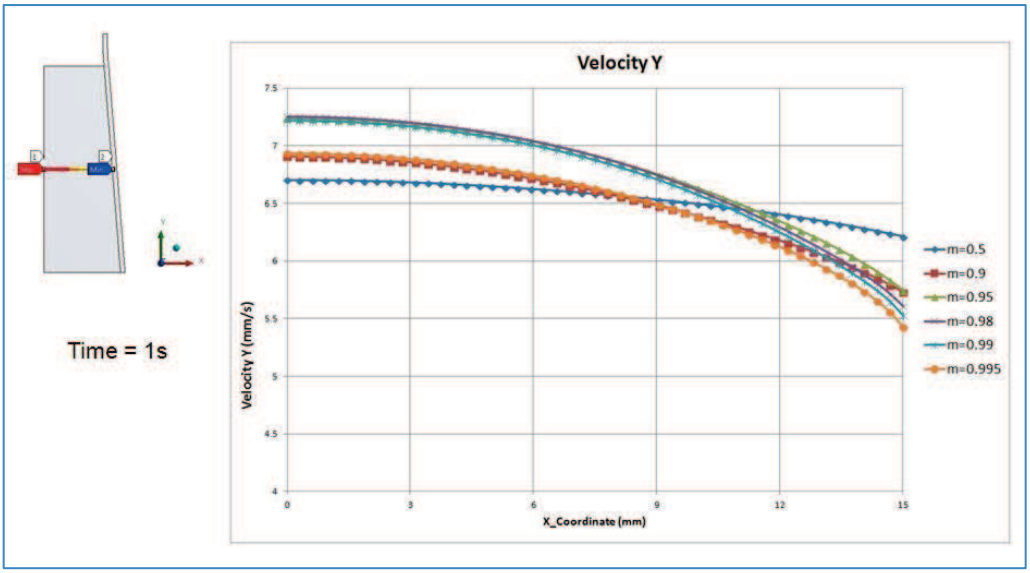

Figure 9. Distribution of the vertical velocities alongh the highlited path of the domain for different values of the Tresca parameter m for the rigid-perfectly plastic material.

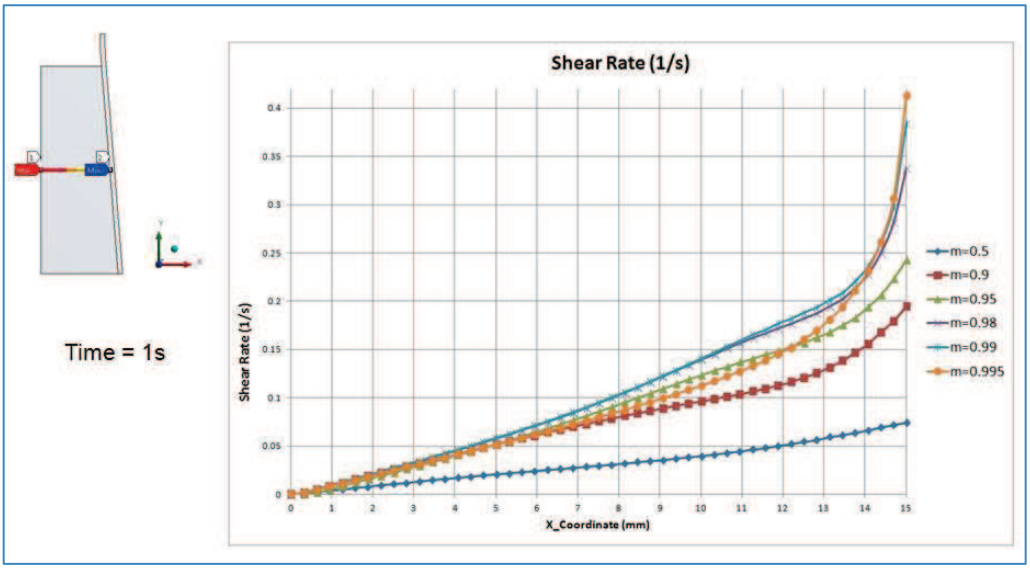

Figure 4. Distribution of the shear component of the strain rate along the same middle part of the channel for different values of the Tresca parameter m for the rigid-perfectly plastic material.

Figure shows how the shear component of the strain rate depends on the path position. When the path is chosen closer to the upper border of the formed domain where the material undergos more sevire plastic deformation, the global trend becomes more complex. However, the curves still presrerve the main feature: the highest values of the strain rate are achived near the mold wall and it becomes singular for the limiting case m = 1.

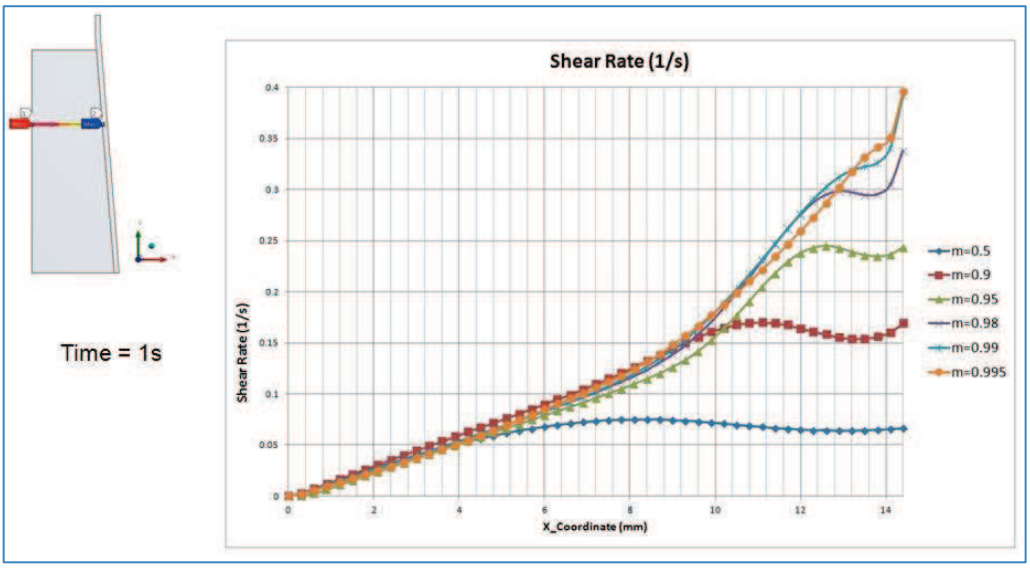

Figure 11. Distribution of the shear component of the strain rate along the other path in the channel for different values of Tresca parameter m for the rigid-perfectly plastic material.

4.2 Plastic model with hardening.

Material considered in the previous subsection was an ideal material: rigid-perfectly plastic. However, *green body* in a compaction process normally demonsttate hardening effect after yielding has occurred, and, as regards to the elastic part, can have Young modulus much lower than supposed previously. For this reason, further analysis was performed using material called

- material 2: the same Young modulus for the elestic part as in the previous model and linear kinematic hardening after yielding: $k_y = k_0 + k_1\varepsilon$, where $k_0 = 50$ MPa, $k_1 = 100$ MPa, and ε is the equivalent strain;
- material 3: with the Young modulus smaller than in two previous material models $E_3 = 2 \cdot 10^4$ MPa and the same linear kinematic hardening after yielding as in the material 2.

Results for the vertical velocity and the shear component of the strain rate tensor along the middle path of the extrusion domain and computed for these two materials are shown in Figure – Figure 15. For such materials, solution with maximum friction at th boundary does not exist and sticking has to occure wne $m = 1$. Indeed, ihe solutions were obtained foe a bit smaller values of the friction parameter m. Behaviour of the solution in cases of these more “realistic” materials are even more complex than for the rigid-perfectly plastic material 1 in the regions clode to the upper or lower entrances of the extrusion domain.

The same tendency for the shear component of the strain rate near the mold wall is also observed in these two cases.

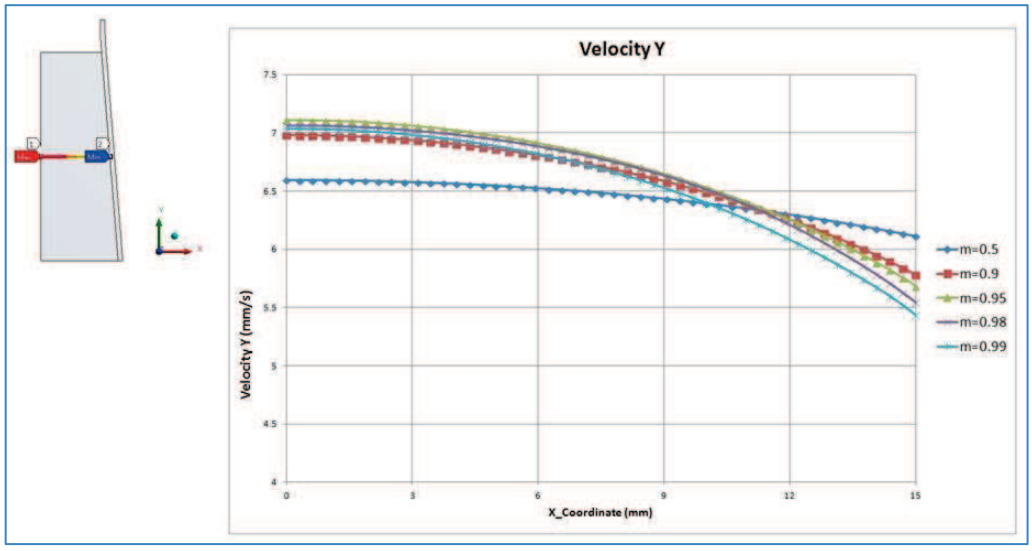

Figure 12. Distribution of the vertical velocities alongh the highlited path of the domain for different values of the Tresca parameter *m* for the material 2 case.

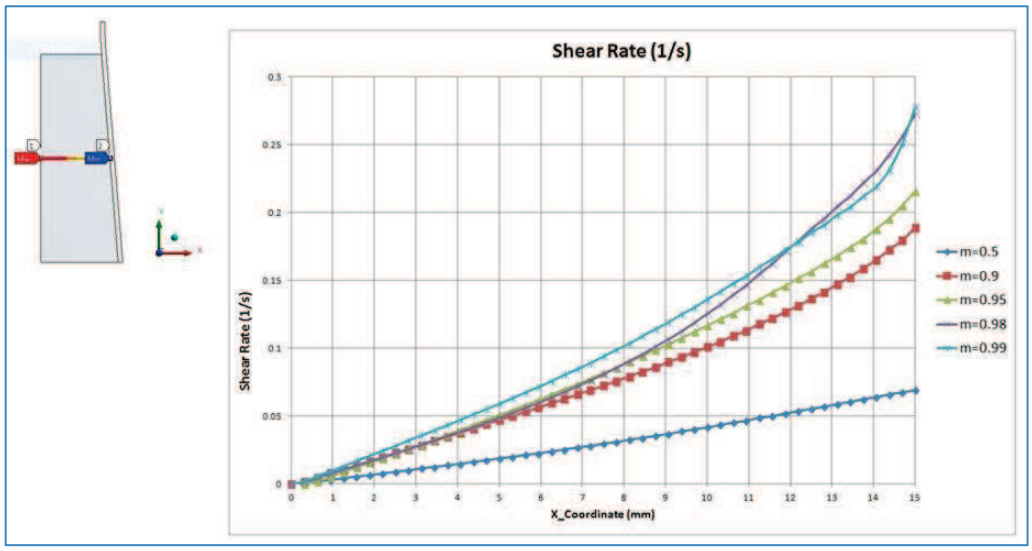

Figure 13. Distribution of the shear component of the strain rate along the middle path of the channel for different values of Tresca parameter *m* for material 2 case.

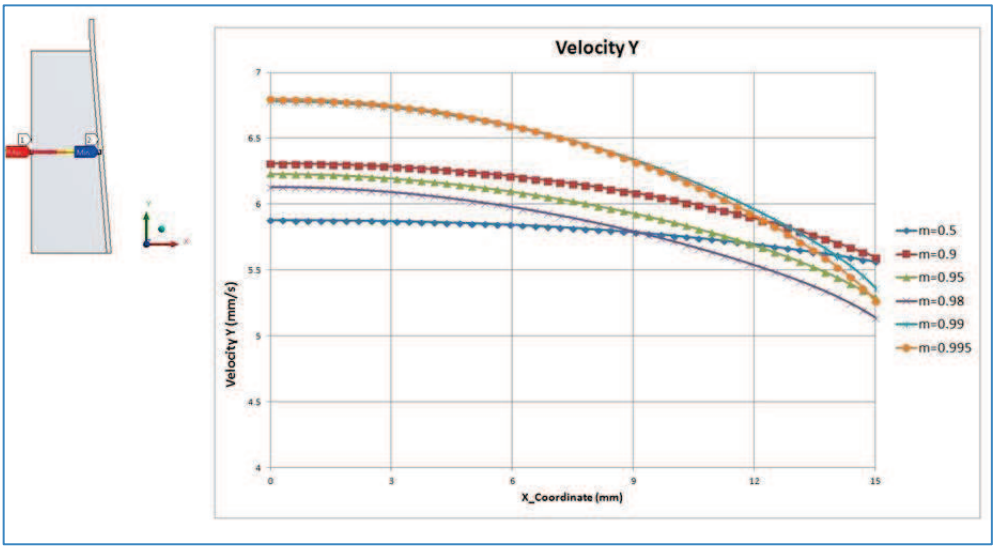

Figure 14: Distribution of the vertical velocities alongh the highlited path of the domain for different values of the Tresca parameter *m* for the Material 3 case.

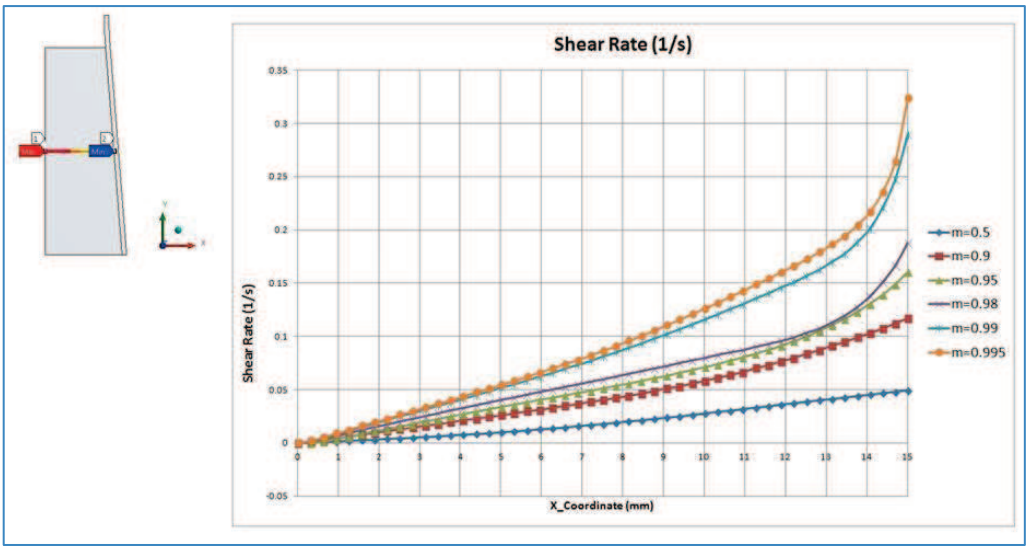

Figure 15: Distribution of the shear component of the strain rate along the middle path of the channel for different values of Tresca parameter *m* for Material 3 case.

5. Conclusions

ANSYS structural program can be used for forming process in ceramic using Tresca friction law. For the given geometry, entrance boundary conditions and the analyzed materials, one can obtain meaningful results for the friction parameter *m* close enough to its maximal value provided that:

- Appropriate mesh dimension is used, better with quadratic elements and finer mesh near the mold wall;
- Small time steps are imposed above all at the beginning of simulation;

- Appropriate macro or user subroutine is built to write parameter TAUMAX in tabular format and to allow restart of analysis at each time steps.

Calculations could be easily extended to more complex geometries if ANSYS developers implement the Tresca law directly into software alongside with other friction laws. In its present form, ANSYS cannot compute the limiting case of maximal friction law (m = 1) with its standard settings and elements types.

The maximum shear stress condition could be probably implemented into ANSYS directly if the developers adopt the respective special singular element. This task has been already recognized as important (see [33]). This would allow researchers to test the concept of the strain rate intensity factor recently proposed in [34, 35].

Acknowledgements: MF and WM are thankful for support from the FP7 PEOPLE Marie Curie projects INTERCER2 (PIAP-GA-2011-286110-INTERCER2) and PARM2 (PIAP-GA-2012-284544-PARM2), respectively

6. Bibliography

[1] J.S. Reed. Principles of Ceramic Processing, (1995) Wiley & Sons, New York.

[2] K.G. Ewsuk. Compaction science and technology. MRS Bull. 22 (1997) 14-16.

[3] S.J. Glass and K.G. Ewsuk. Ceramic powder compaction. MRS Bull. 22, (1997) 24-28.

[4] A.R. Cooper, L.E. Eaton. Compaction behavior of several ceramic powders. J. Am. Ceram. Soc. 45 (1962) 97-101.

[5] S.B. Brown, G.A. Weber. A constitutive model for the compaction of metal powders. Mod. Dev. Powder Metall. 18-21 (1988) 465-476.

[6] S.B. Brown, G. Abou-Chedid. Yield behaviour of metal powder assemblages, J. Mech. Phys. Solids 42 (1994) 383-399.

[7] J. Oliver, S. Oller and J.C. Cante. A plasticity model for simulation of industrial powder compaction processes. Int. J. Solids Struct. 33 (1996) 3161-3178.

[8] I. Aydin, B. Briscoe, N. Ozkan. Modeling of powder compaction: a review. MRS Bull. 22, (1997) 45-51

[9] J. Brandt, L.A. Nilsson. constitutive model for compaction of granular media, with account for deformation induced anisotropy. Mech. Cohesive-Frict. Mater. 4, (1999) 391-418.

[10] D. Bigoni, A. Piccolroaz. Yield criteria for quasibrittle and frictional materials. Int. J. Solids Struct. 41, (2004) 2855-2878

[11] A. Piccolroaz, D. Bigoni, A. Gajo, An elastoplastic framework for granular materials becoming cohesive through mechanical densification. Part I – small strain formulation, European Journal of Mechanics A/Solids 25, (2006), 334–357

[12] F. Bosi, A. Piccolroaz, M. Gei, F. Dal Corso, A. Cocquio, D. Bigoni, Experimental investigation of the elastoplastic response of aluminum silicate spray dried powder during cold compaction. Journal of the European Ceramic Society 34, (2014), 2633–2642

[13] S. Stupkiewicz, A. Piccolroaz, D. Bigoni. Elastoplastic coupling to model cold ceramic powder compaction. Journal of the European Ceramic Society, 34 (2014) 2839-2848.

[14] A. Piccolroaz, D. Bigoni. Yield criteria for quasibrittle and frictional materials: a generalization to surfaces with corners. International Journal of Solids and Structures, 46 (2009) 3587-3596.

[15] S. Stupkiewicz, R. Denzer, A. Piccolroaz, D. Bigoni. Implicit yield function formulation for granular and rock-like materials. *Computational Mechanics*, **54**, (2014) 1163-1173.

[16] Bowden, F.P. and Tabor, D. (1950) The friction and lubrication of solids. Oxford Science Publ., Clarendon Press.

[17] S. Alexandrov, O. Richmond. Singular plastic flow field near surfaces of maximum friction stress, International Journal of Nonlinear Mechanics, 36 (2001) 1-11.

[18] S. Alexandrov Singular solutions in an axisymmetric flow of a medium obeying the double shear model. J. Appl. Mech. Techn. Physics. 46 (5) (2005) 766-771.

[19] S. Alexandrov and R. Goldstein. Plastic flow in a conical channel: qualitative features of the solutions under different yield conditions. J. Appl. Maths Mechs. 71 (1) (2007) 111-119.

[20] S. Alexandrov and N. Alexandrova. On the maximum friction law in viscoplasticity, Mech. Time-Depend. Mater. 4 (1) (2000) 99-104.

[21] S. Alexandrov, G. Mishuris. Qualitative behaviour of viscoplastic solutions in the vicinity of maximum-friction surfaces, J. Eng. Math., 65, (2009), 143 – 156.

[22] S. Alexandrov, W. Miszuris. On the transition of qualitative behaviour between rigid perfectly plastic and viscoplastic solutions, J. Eng. Math., (2015) DOI: 10.1007/s10665-015-9797-7

[23] S Alexandrov, G Mishuris, W Miszuris, RE Sliwa. On the dead-zone formation and limit analysis in axially symmetric extrusion. International Journal of Mechanical Sciences, 43 (2) (2001), 367-379

[24] S. Alexandrov, W. Miszuris. Heat generation in plane strain compression of a thin rigid plastic layer. Acta Mechanica, (2015), DOI: 10.1007/s00707-015-1499-8

[25] R.A. Thompson. Mechanics of powder pressing: II, Finite-element analysis of end-capping in pressed green powders. Am. Ceram. Soc. Bull. 60 (1981) 244-247.

[26] H. Zipse. Finite-element simulation of die pressing and sintering of a ceramic component. J. Eur. Ceram. Soc. 17, (1997) 1707-1713.

[27] I. Aydin, B. Briscoe and K.Y. Sanliturk. Dimensional variation of die-pressed ceramic green compacts: comparison of a finite element modelling with experiment. J. Eur. Ceram. Soc. 17 (1997) 1201-1212.

[28] A.K. Ariffin, D.T. Gethin and R.W. Lewis. Finite element simulation and experimental validation for multilevel powder compact. Powder Metallurgy 41 (1998) 189-197.

[29] J. Brandt and L. Nilsson. FE-simulation of compaction and solid-state sintering of cemented carbides. Mech. Cohesive-Frict. Mater. 3 (1998) 181-205.

[30] P. Redanz. Numerical modelling of the powder compaction of a cup. Eur. J. Mech., A Solids 18 (1999) 399-413.

[31] M. Sonato, A. Piccolroaz, W. Miszuris, G. Mishuris. General transmission conditions for thin elasto-plastic pressure-dependent interphase between dissimilar materials. International Journal of Solids and Structures, 64-65 (2015) 9-21.

[32] ANSYS Help version 15.0, Ansys Inc. – 2014

[33] S. Alexandrov, C.-Y. Kuo, Y.-R. Jeng. A numerical method for determining the strain rate intensity factor under plane strain conditions. Continuum Mechanics and Thermodynamics, (2015) 1-16, DOI: 10.1007%2Fs00161-015-0436-3.

[34] S.E. Aleksandrov, E.A. Lyamina. Strain rate intensity factors for a plastic material layer compressed between cylindrical surfaces. Mechanics of Solids, 48 (6) (2013) 636-648

[35] E. Lyamina, S. Alexandrov. Application of the Strain Rate Intensity Factor to Modeling Material Behavior in the Vicinity of Frictional Interfaces. In "Trends in Computational Contact Mechanics", Volume 58 of the series Lecture Notes in Applied and Computational Mechanics, 291-320